Electronic transport of $(In_{1-x}Fe_x)_2O_{3-v}$ magnetic semiconductor and Fe–In_2O_3 granular films in the presence of electronic screening

2007 J. Phys.: Condens. Matter 19 326206

(http://iopscience.iop.org/0953-8984/19/32/326206)

IOP PUBLISHING JOURNAL OF PHYSICS: CONDENSED MATTER

J. Phys.: Condens. Matter **19** (2007) 326206 (8pp) doi:10.1088/0953-8984/19/32/326206

Electronic transport of $(In_{1-x}Fe_x)_2O_{3-v}$ magnetic semiconductor and Fe–In_2O_3 granular films in the presence of electronic screening

Y F Tian, Shi-shen Yan[1], Y P Zhang, P F Xing, G L Liu, Y X Chen and L M Mei

School of Physics and Microelectronics, and National Key Laboratory of Crystal Materials, Shandong University, Jinan, Shandong 250100, People's Republic of China

E-mail: shishenyan@yahoo.com

Received 11 March 2007, in final form 12 June 2007
Published 16 July 2007
Online at stacks.iop.org/JPhysCM/19/326206

Abstract

$(In_{1-x}Fe_x)_2O_{3-v}$ amorphous ferromagnetic semiconductor films were prepared by sputtering under thermal non-equilibrium conditions, and their corresponding Fe–In_2O_3 granular films were obtained by annealing. Unexpectedly, they both showed Mott variable range hopping behavior in the low temperature range, indicating that the interaction between the carriers can be neglected in the hopping process. For a system with a high carrier concentration the negligible interaction between the carriers was due to the electronic screening effect on the long range Coulomb interaction. The magnetoresistance in $(In_{1-x}Fe_x)_2O_{3-v}$ magnetic semiconductor and Fe–In_2O_3 granular films is also discussed. However, electronic transport through intergrain tunneling was not observed in the annealed Fe–In_2O_3 granular films.

1. Introduction

In recent years, intense researches have been carried out in the field of magnetic semiconductors due to their potential spintronics applications. Various electrical transport [1–9] and ferromagnetic phenomena [10–15] in such disordered systems have been extensively studied because of their significant importance in fundamental physics. For most magnetic semiconductors, the solubility of doped magnetic ions in the host semiconductor lattice is very low and the carrier density is hard to tune. Magnetic semiconductors with a high solubility of transition metal ions and tunable carrier density are highly desirable for achieving a high Curie temperature. In this sense, a magnetic semiconductor based on an In_2O_3 host is a good

[1] Address for correspondence: School of Physics and Microelectronics, Shandong University, Jinan, Shandong 250100, People's Republic of China.

candidate since In_2O_3 is a wide band gap semiconductor with a cubic bixbyite crystal structure which can become a highly conducting n-type semiconductor with the introduction of oxygen deficiencies or Sn doping [11–15]. An encouragingly high thermodynamic solubility of as much as 20% for Fe ions in In_2O_3 has been reported [13]. However, experimental results for Fe-doped In_2O_3 magnetic semiconductors reported by different groups are different and even contradictory [13–15].

Recently, spin dependent Efros and Shklovskii variable range hopping (VRH) was observed in $Zn_{1-x}Co_xO$ [16] and $Ti_{1-x}Co_xO_2$ [17] magnetic semiconductor films with high Co concentration. This was attributed to the presence of electron–electron Coulomb interaction and spin–spin exchange interaction between the carriers. Furthermore, the transformation of electrical transport from Efros and Shklovskii VRH to 'hard gap' resistance was experimentally observed in a low temperature range as the Fe composition in the $Zn_{1-x}Fe_xO_{1-v}$ ferromagnetic semiconductor increased [18]. Even less is known about the electrical transport and magnetoresistance of $(In_{1-x}Fe_x)_2O_{3-v}$ ferromagnetic semiconductor films with high Fe concentration and Fe–In_2O_3 granular films. In this paper, $(In_{1-x}Fe_x)_2O_{3-v}$ amorphous ferromagnetic semiconductor films with high Fe compositions were synthesized, and Fe–In_2O_3 granular films were obtained by annealing. In contrast to Efros and Shklovskii VRH and 'hard gap' transport observed in $Zn_{1-x}Co_xO$, $Ti_{1-x}Co_xO_2$ and $Zn_{1-x}Fe_xO_{1-v}$ magnetic semiconductor films [18, 19], Mott VRH was observed in both as-deposited $(In_{1-x}Fe_x)_2O_{3-v}$ ferromagnetic semiconductors and annealed Fe–In_2O_3 granular films, and was attributed to an electronic screening effect on the long range Coulomb interaction.

2. Experiment

The nominal [Fe 0.5 nm/In_2O_3 y nm]$_{60}$ structures were prepared on a water-cooled glass substrate (thermal non-equilibrium process) by alternately depositing very thin Fe and In_2O_3 bilayers for 60 periods in a flow of Ar gas and the remanent O_2 background with good reproducibility. The growth rate of Fe and In_2O_3 layers is 0.25 Å s^{-1} and 0.13 Å s^{-1}, respectively. The method used here is similar to that used in [16]. Due to atomic interdiffusion, the nominal structures formed metastable $(In_{1-x}Fe_x)_2O_{3-v}$ amorphous ferromagnetic semiconductor films with different Fe compositions. Since the solubility of Fe in In_2O_3 in a thermal equilibrium state is lower than that in the as-deposited films, the as-prepared films can further develop into Fe–In_2O_3 granular composite films after proper annealing in a vacuum (such as annealing at 400 °C for 1 h and 450 °C for 2 h).

Magnetic properties were measured by a superconducting quantum interference device (SQUID) with a magnetic field in the film plane. The electrical transport properties were measured in a Van der Pauw configuration by adding a Keithly 2400 as the current source and a Keithly 2182 as a voltage meter in the SQUID machine with a magnetic field in the film plane or without a magnetic field.

3. Experimental results and discussion

Crystal structures of the as-deposited and post-annealing films were analysed by x-ray diffraction (XRD) using Cu Kα irradiation. Figure 1(a) is a XRD pattern of the as-deposited $(In_{0.31}Fe_{0.69})_2O_{3-v}$ film. No diffraction peak was observed except for the wide peak of the glass substrate, indicating that the film is in an amorphous state. Figures 1(b) and (c) are XRD results for the $(In_{0.31}Fe_{0.69})_2O_{3-v}$ film annealed at 400 and 450 °C. It was obvious that Fe and In_2O_3 diffraction peaks appeared in the annealed samples, but no Fe_3O_4 and Fe_2O_3 compounds were found. Therefore we believe that in the annealing process phase segregation occurs along

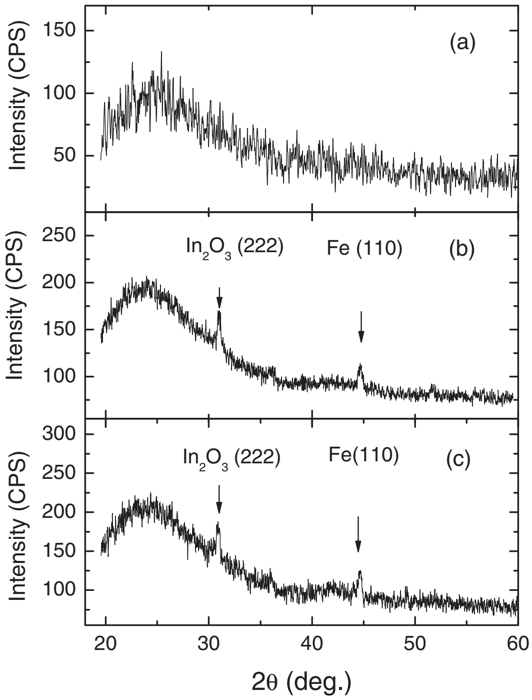

Figure 1. XRD patterns of the $(In_{0.31}Fe_{0.69})_2O_{3-v}$ films: (a) as-deposited magnetic semiconductor film, (b) granular film annealed at 400 °C for 1 h, and (c) granular film annealed at 450 °C for 2 h.

with the crystallization such that the amorphous films are transformed into crystalline Fe-doped In_2O_3 with ferromagnetic Fe inclusions.

Figures 2(a) and (b) show the temperature dependence of the sheet resistance of two as-deposited films, $(In_{0.31}Fe_{0.69})_2O_{3-v}$ and $(In_{0.39}Fe_{0.61})_2O_{3-v}$. The sheet resistance decreases with increasing temperature, which is a typical feature of the semiconductor resistance. Although the sheet resistance strongly depends on the sample composition, the good linear relationship between ln R and $T^{-1/4}$ in the low temperature range indicated that the electronic transport mechanism was Mott VRH. This behavior indicated that the interaction between the carriers can be neglected in the hopping process. By contrast, in similar magnetic semiconductor films such as $Zn_{1-x}Co_xO$ [16], $Ti_{1-x}Co_xO_2$ [17] and $Zn_{1-x}Fe_xO_{1-v}$ [18] prepared by the same method, electronic transport shows Efros and Shklovskii VRH and/or hard gap resistance, where the electron–electron Coulomb interaction and the hard gap potential played a crucial role in the hopping transport. On the other hand, it is noticed that the resistivity (3.8×10^{-5} Ω m) of $(In_{0.31}Fe_{0.69})_2O_{3-v}$ film was 2 or 3 orders lower than that of $Zn_{0.28}Co_{0.72}O$ (7.4×10^{-2} Ω m), $Ti_{0.24}Co_{0.76}O_2$ (8.73×10^{-3} Ω m), and $Zn_{0.3}Fe_{0.7}O_{1-v}$ (5.1×10^{-3} Ω m) films at 5 K. The much less resistivity in $(In_{0.31}Fe_{0.69})_2O_{3-v}$ films may originate from higher carrier concentration, larger localization length of the carriers, and/or lower hopping potential in the $(In_{1-x}Fe_x)_2O_{3-v}$ ferromagnetic semiconductors. It is very interesting to notice that the electronic transport in such a $(In_{1-x}Fe_x)_2O_{3-v}$ ferromagnetic semiconductor system can be well described by Mott VRH without considering the interaction between the carriers.

In the following, we gave an explanation of the experimental results by taking into account the screening effect on the long range Coulomb interaction. A mathematical analysis shows

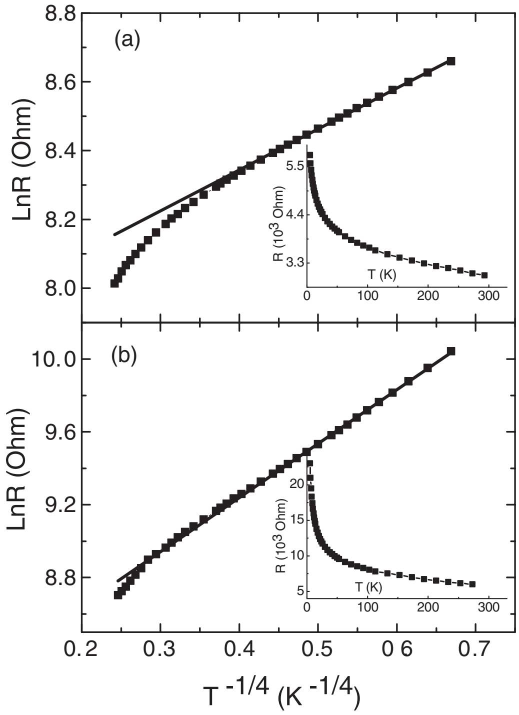

Figure 2. The dependence of $\ln R$ on $T^{-1/4}$ for $(In_{1-x}Fe_x)_2O_{3-v}$ ferromagnetic semiconductor films with different Fe compositions: (a) $(In_{0.31}Fe_{0.69})_2O_{3-v}$ and (b) $(In_{0.39}Fe_{0.61})_2O_{3-v}$. Squares represent the experimental data and solid lines are theoretical fittings according to Mott VRH. The inset curves show the temperature dependence of the sheet resistance.

that an impurity ion in a semiconductor is shielded by oppositely charged carriers as part of the neutralization process. Because of the screening effect of the shielding electrons or holes, the Coulomb field around the impurity state becomes short range. Beyond a certain distance (the screening length), the interaction between two localized states becomes negligible. The screening length is proportional to the square root of temperature and inversely proportional to the square root of carrier density [20]. Since $(In_{1-x}Fe_x)_2O_{3-v}$ the ferromagnetic semiconductor has a lower resistivity, and it is reasonable to believe that it has high carrier concentration. So the $(In_{1-x}Fe_x)_2O_{3-v}$ films should have a relatively small screening length in the low temperature range. In addition, the hopping length of Mott VRH is proportional to $T^{-1/4}$ and it can be very large in the low temperature range. Therefore, for the long range hopping process beyond the electronic screening length, the Coulomb interaction between the initial and final states can be neglected and Mott VRH for noninteracting carriers was discovered instead of Efros and Shklovskii VRH for interacting carriers.

Figures 3(a) and (b) show the temperature dependence of sheet resistance of the annealed Fe–In_2O_3 granular films. It is well known that most metal–insulator granular systems show a linear relation between $\ln R$ and $T^{-1/2}$ in a wide temperature range [3], and this linear relation was even suggested as a rapid method for determining the presence of clustering in magnetically doped semiconductor systems [6]. Unexpectedly, the annealed Fe–In_2O_3 granular films still show Mott VRH in the low temperature range, rather than the intergrain tunneling transport usually observed in the granular systems [3].

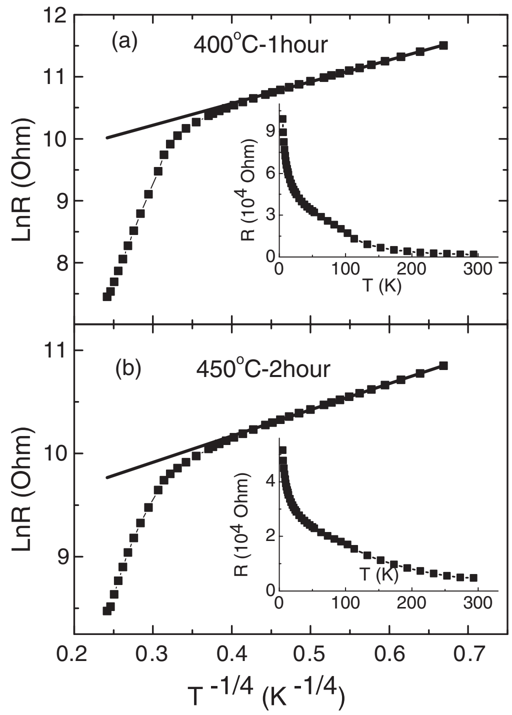

Figure 3. The dependence of ln R on $T^{-1/4}$ for annealed $(In_{0.31}Fe_{0.69})_2O_{3-v}$ films at (a) 400 °C for 1 h and (b) 450 °C for 2 h. Squares stand for the experimental data and solid lines are theoretical fittings according to Mott VRH. The inset curves are the temperature dependence of the sheet resistance.

The unexpected Mott VRH in the Fe–In_2O_3 granular films can be understood by considering the following factors. First, in the low temperature range the charging energy of the small Fe clusters should be much larger than the thermal energy. In this case the electron tunneling between the small Fe clusters was highly suppressed. The small size of the Fe clusters can be known from the weak and wide Fe(110) peak of the XRD patterns as shown in figure 1. Second, strictly speaking, the Fe–In_2O_3 granular films should be Fe–$(In_{1-x}Fe_x)_2O_{3-v}$ composite, due to the relatively large solubility of Fe in In_2O_3. The remanent $(In_{1-x}Fe_x)_2O_{3-v}$ matrix after annealing can provide additional transport paths through VRH between localized defect states in the matrix. As a result, in the Fe–$(In_{1-x}Fe_x)_2O_{3-v}$ granular films the carriers prefer to transport through VRH between localized defect states rather than tunneling between small Fe clusters. However, at high temperatures the electrical transport deviated from the Mott VRH behavior because the thermal energy is high and allows other electrical transport paths, such as nearest neighbor hopping, direct tunneling between Fe clusters and so on.

The M–H and R–H curves of the as-deposited $(In_{0.31}Fe_{0.69})_2O_{3-v}$ ferromagnetic semiconductor films are shown in figures 4(a) and (b), respectively. The ferromagnetism is clearly shown by the coercivity, remanence and low saturation field in figure 4(a). In figure 4(b), the R–H curve shows a butterfly-like shape and the two resistance peaks correspond to the measured coercive field (±1400 Oe). The resistance tends to be a saturation value as the magnetic moment tends to saturate with increasing the field. No detectable difference in the magnetoresistance was observed for different orientations of the magnetic field in the film plane with respect to the current flow (no anisotropic magnetoresistance in the film plane). Almost

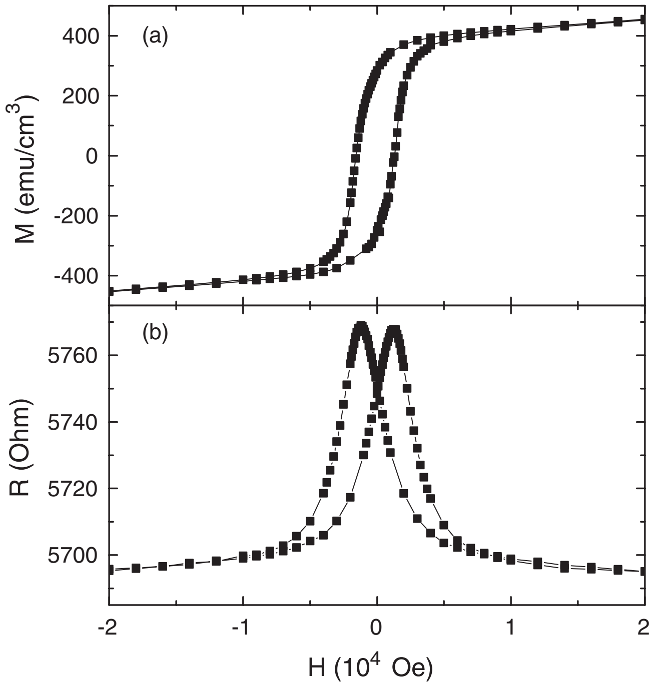

Figure 4. The magnetic hysteresis loop (a) and the magnetoresistance (b) of the as-deposited $(In_{0.31}Fe_{0.69})_2O_{3-v}$ film measured at 5 K with the magnetic field in the film plane.

the same small magnetoresistance ratio was observed for the magnetic field parallel to the film plane and perpendicular to the film plane. This means that the magnetoresistance due to the orbital effect was negligible. Analogously to the negative MR due to spin dependent Efros and Shklovskii VRH observed in $Zn_{1-x}Co_xO$ and $Ti_{1-x}Co_xO_2$ [19], this negative MR in $(In_{1-x}Fe_x)_2O_{3-v}$ can be explained by spin dependent Mott VRH.

Figures 5(a) and (b) show the *M–H* and *R–H* curves of the annealed granular films measured with the magnetic field in the film plane. Although the electronic transport mechanism was the same for $(In_{1-x}Fe_x)_2O_{3-v}$ amorphous ferromagnetic semiconductor and Fe–$(In_{1-x}Fe_x)_2O_{3-v}$ granular films, the MR behavior was quite different. Although an obvious hysteresis loop was observed in the *M–H* curve, no hysteresis behavior in *R–H* curve was found for the granular films. This revealed that the variation of the resistance with the applied magnetic field had no correlation to the reversal of the magnetization in Fe clusters. It may be useful to mention that the observed magnetic transport properties are very similar to the reported experimental results in dilute $Zn_{1-x}Fe_xO$, $Zn_{1-x}Co_xO$ magnetic semiconductors [7–9]. This further indicates that the observed MR in the annealed granular films is not due to spin dependent tunneling between Fe grains. However, the peculiar magnetoresistance in the annealed films is not well understood. Further research work on magnetic transport is desirable.

4. Conclusions

In conclusion, both $(In_{1-x}Fe_x)_2O_{3-v}$ ferromagnetic semiconductor films and their corresponding Fe–In_2O_3 granular films show Mott VRH behavior in the low temperature range,

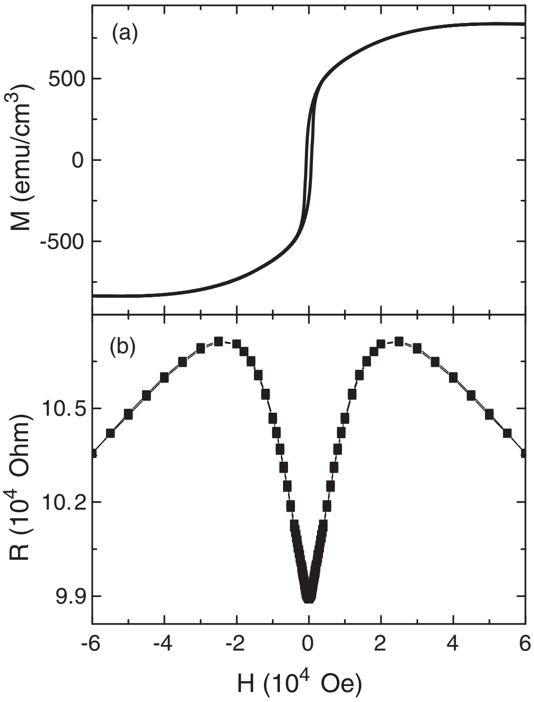

Figure 5. The magnetic hysteresis loop (a) and field dependence of sheet resistance (b) of the $(In_{0.31}Fe_{0.69})_2O_{3-v}$ film annealed at 400 °C for 1 h measured at 5 K.

indicating that interaction between the carriers can be neglected in the hopping process. For a system with a high carrier concentration, the negligible interaction between the carriers is caused by the electronic screening effect on the long range Coulomb interaction. However, electronic transport through intergrain tunneling was not observed in the annealed Fe–In_2O_3 granular films.

Acknowledgments

This work was supported by 973 project, an NSF grant and the NCET fund.

References

[1] Mott N F 1968 *J. Non-Cryst. Solids* **1** 1
[2] Efros A L and Shklovskii B I 1975 *J. Phys. C: Solid State Phys.* **8** L49
[3] Sheng P, Abeles B and Arie Y 1973 *Phys. Rev. Lett.* **31** 44
[4] Nissim M and Rosenbaum R L 1989 *Phys. Rev.* B **10** 10629
[5] Peleckis G, Wang X L and Dou S X 2006 *Appl. Phys. Lett.* **89** 025501
[6] Kennedy R J, Stampe P A, Hu E, Xiong P, von Molnár S and Xin Y 2004 *Appl. Phys. Lett.* **84** 2832
[7] Xu Q Y, Hartmann L, Schmidt H, Hochmuth H, Lorenz M, Schmide-Grund R, Spemann D and Grundmann M 2006 *J. Appl. Phys.* **100** 013904
[8] Stamenov P, Venkatesan M, Dorneles L S, Maude D and Coey J M 2006 *J. Appl. Phys.* **99** 08M124
[9] Han S-J, Song J W, Yang C H, Park S H, Park J H, Jeong Y H and Rhie K W 2002 *Appl. Phys. Lett.* **81** 4212
[10] Philip J, Punnoose A, Kim B I, Reddy K M, Layne S, Holmes J O, Satpati B, Leclair P R, Santos T S and Moodera J S 2006 *Nat. Mater.* **5** 298

[11] Philip J, Theodoropoulou N, Berera G, Moodera J S and Satpati B 2004 *Appl. Phys. Lett.* **85** 777
[12] Hong N H, Sakai J, Huong N T and Brizé V 2005 *Appl. Phys. Lett.* **87** 102501
[13] He J, Xu S F, Yoo Y K, Xue Q Z, Lee H C, Cheng S F, Xiang X D, Dionne G F and Takeuchi I 2005 *Appl. Phys. Lett.* **86** 052503
[14] Yoo Y K, Xue Q Z, Lee H C, Cheng S F, Xiang X D, Dionne G F, Xu S F, He J, Chu Y S, Preite S D, Lofland S E and Takeuchi I 2005 *Appl. Phys. Lett.* **86** 042506
[15] Peleckis G, Wang X L and Dou S X 2006 *Appl. Phys. Lett.* **88** 132507
[16] Yan S S, Ren C, Wang X, Yan X, Zhou Z X, Mei L M, Ren M J, Chen Y X, Liu Y H and Garmestani H 2004 *Appl. Phys. Lett.* **84** 2376
[17] Song H Q, Mei L M, Yan S S, Ma X L, Liu J P, Yong Y and Zhang Z 2006 *J. Appl. Phys.* **99** 123903
[18] Tian Y F, Yan S S, Zhang Y P, Song H Q, Ji G, Liu G L, Chen Y X, Mei L M, Liu J P, Altuncevahir B and Chakka V 2006 *J. Appl. Phys.* **100** 103901
[19] Yan S S, Liu J P, Mei L M, Tian Y F, Song H Q, Chen Y X and Liu G L 2006 *J. Phys.: Condens. Matter* **18** 10469
[20] Kwon Young D 2006 *Phys. Rev.* B **73** 165210